

Simulations study of events from tau production and decay

Sumanta Pal^{*†}

University of Sheffield

E-mail: sumanta.pal@sheffield.ac.uk

D. Indumathi

The Institute of Mathematical Sciences

E-mail: indu@imsc.res.in

A magnetised Iron-CALorimeter (ICAL) detector is proposed to be set up in the India-based Neutrino Observatory (INO) to study atmospheric neutrino oscillations with a view to make precise measurements of neutrino oscillation parameters. Atmospheric neutrinos produce muons through CC interactions in the ICAL detector which is the dominant signal. Tau neutrinos are produced mainly in the upward going atmospheric neutrinos due to the neutrino flavour oscillations. These ν_τ 's on interactions with the detector target mass produce τ 's and hadrons. Tau particles are short lived particles and a major fraction decays to hadrons. These two sets of hadrons add to give an event that mimics a high energy NC event and can be detected as an excess over the background NC expectation. The significance of this tau contribution has been determined through a χ^2 analysis. Our simulation study shows that there is a possibility to measure the signature for tau production through this indirect channel.

*16th International Workshop on Neutrino Factories and Future Neutrino Beam Facilities - NUFAC2014,
25 -30 August, 2014*

University of Glasgow, United Kingdom

^{*}Speaker.

[†]Present affiliation.

1. Atmospheric neutrino flux

The atmospheric neutrino flux is taken from Ref. [1, 2, 3, 4]. The neutrino flux at SuperK is considered so far for various physics analysis by the INO collaboration. Preliminary flux data at INO site is also available [1]; the differences are mostly in the low energy region due to latitude effects and are negligible for tau analysis. Beyond 3 GeV there is no appreciable change between two fluxes. The input consists of ν_μ , ν_e , $\bar{\nu}_\mu$ and $\bar{\nu}_e$ spectra distributed over E_ν , $\cos\theta$, and ϕ , where θ is the zenith angle, ϕ is the azimuthal angle and E_ν is the energy of the incoming neutrino. The energy range for E_ν is from 0.1 GeV to 10 TeV as given in the Honda flux [1]. In this particular study, we have included contributions from E_ν in the range of 3 GeV to 100 GeV (considering energy threshold for the tau production), where flux is falling at the rate of $E_\nu^{-2.7}$. The neutrino fluxes are symmetric about $\cos\theta$ for $E_\nu > 3.2$ GeV between the up- and down-directions where $\cos\theta = -1$ refers to the up-going neutrinos.

2. Neutrino Oscillations

τ neutrinos can mainly be produced through oscillations; the oscillation probabilities $P_{\mu\tau}$ and $P_{e\tau}$ (and analogous expressions for anti-neutrinos) are relevant here. A detailed discussion on neutrino oscillation probability and its sensitivity to neutrino oscillation parameters for a detector with charge identification capability has been presented in Ref. [5]. To be brief, 3-flavour neutrino oscillation model is considered here. In our analysis we have used the following bench-mark values for the oscillation parameters [6] (Table 1). The density profile of the Earth is taken from the

Parameter	Best-fit value
θ_{12}	33.36°
θ_{23}	45.0°
θ_{13}	9.217°
δ_{CP}	0
δ_{12}	$7.5 (\times 10^{-5} \text{ eV}^2)$
$ \Delta m^2 $	$2.4 (\times 10^{-3} \text{ eV}^2)$

Table 1: The best-fit values of oscillation parameters used in this analysis.

Preliminary Reference Earth Model (PREM) [7] and it is incorporated into the oscillation probability calculation. The neutrino propagation equation in matter is solved numerically to obtain the oscillation probabilities. Details can be found in [5].

3. Neutrino-nucleon cross sections for CC processes

The CC interactions of tau-type neutrinos with the detector target are given by eq. 3.1.

$$\begin{aligned} \nu_\tau + n &\rightarrow \tau^- + p, \\ \bar{\nu}_\tau + p &\rightarrow \tau^+ + n. \end{aligned} \tag{3.1}$$

Since the energies of interest are from a few GeV to 100 GeV, the CC interactions includes quasi-elastic (QE), resonance (Res) and deep inelastic (DIS) processes. In the resonance case, only Δ resonance production has been considered. We consider here double differential cross-sections for tau production which is written in the form,

$$\frac{d\sigma}{dE_\tau d\cos\theta_\tau} = \frac{G_F^2 \kappa^2}{2\pi} \frac{p_\tau}{m_N} \left[\left(2W_1 + \frac{m_\tau^2}{m_N^2} W_4 \right) (E_\tau - p_\tau \cos\theta_\tau) + W_2 (E_\tau + p_\tau \cos\theta_\tau) \pm \frac{W_3}{m_N} (E_\nu E_\tau + p_\tau^2 - (E_\nu + E_\tau) p_\tau \cos\theta_\tau) - \frac{m_\tau^2}{m_N} W_5 \right], \quad (3.2)$$

where G_F is the Fermi constant, $\kappa = m_W^2 / (Q^2 + m_W^2)$ is the propagator factor with the W-boson mass (m_W), p_τ is the magnitude of the 3-momentum of the charged lepton and the W_i are structure functions corresponding to the general decomposition of the hadronic tensor for QE, Res and DIS processes. The detailed expressions for W_i are taken from Ref. [8] where specific structure functions are listed for QE, Res and DIS leading order processes. We define 4-momenta in the laboratory frame for the process, $\nu_\tau(k) + N(p) \rightarrow \tau^-(k') + X(p')$, as k for incoming neutrino, p for target nucleon, k' for outgoing τ and p' for the net hadrons. We also define some Lorentz invariant variables

$$Q^2 = -q^2, \quad q^\mu = k^\mu - k'^\mu, \\ W_X^2 = (p + q)^2. \quad (3.3)$$

Q^2 is the magnitude of the momentum transfer and W_X is the hadronic invariant mass. The separation between Res and DIS is arbitrary and determined by a cut, chosen to be $W_X \geq 1.4$ GeV. The resonance region is chosen as $(m_N + m_\pi) < W_X < 1.4$ where, m_π is the pion mass. For tau interactions we use the CTEQ6 LO set of parton distribution functions (leading order in the α_S) through the LHAPDF (version 5.8.7) interface.

The tau production is very much in the forward direction with respect to the incoming neutrinos and available phase space is also restricted by the kinematics. More phase space is available for forward going taus as can be seen in Figure 1 where the final hadronic mass ($W_X \geq m_N$) is plotted as a function of E_τ for a fixed energy of $E_\nu = 10$ GeV for different opening angles $\theta_{\tau\nu} \leq 25^\circ$. The cross sections are computed in the frame where incident neutrino direction defines the z -axis and then the results are boosted into the lab frame. The integrated cross-sections is dominated by the DIS process and contribution from anti-neutrinos to the total cross-sections is almost half compared to the neutrinos (Figure 2).

4. Distribution of τ events

The expected number of tau-leptons in the ICAL detector (50 kton) in 5 years exposure are obtained by integrating¹ eq. 4.1. Total (117 ± 0.85) τ^- and (45 ± 0.33) τ^+ are estimated in the upward-going direction ($-1 \leq \cos\theta \leq 0$), whereas in the downward-going direction, oscillation effect is almost absent and so there are no tau events. The distribution of tau-lepton events, as

¹kVegas Monte-Carlo multidimensional integrator is used through the ROOT interface.

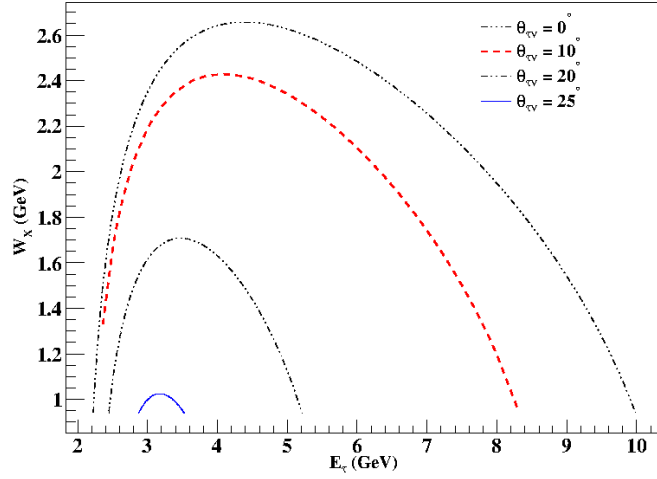


Figure 1: The invariant mass distributions for various opening angles for a fixed value of $E_\nu = 10$ GeV. Note that physically $W_X \geq m_N$, the nucleon mass.

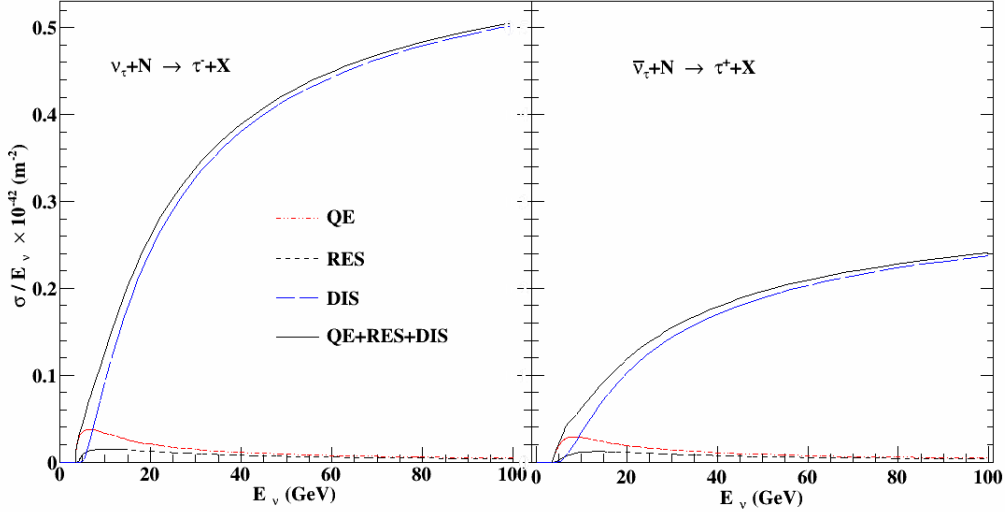


Figure 2: Total cross-sections for the individual processes (QE, Res and DIS) and all together are shown for neutrino (left panel) and anti-neutrino (right panel) interactions.

obtained for the ICAL, is given in Table 2.

$$\begin{aligned}
 N_\tau = N_T \times T \times \int_{E_\nu, \cos \theta_\nu, \phi_\nu} dE_\nu d \cos \theta_\nu d\phi_\nu \left(\frac{d\Phi_{\nu_\mu}}{dE_{\nu_\mu} d \cos \theta_{\nu_\mu} d\phi_{\nu_\mu}} P_{\mu\tau} + \frac{d\Phi_{\nu_e}}{dE_{\nu_e} d \cos \theta_{\nu_e} d\phi_{\nu_e}} P_{e\tau} \right) \\
 \times \int_{E_\tau^{min}}^{E_\tau^{max}} dE_\tau \int_{\cos \theta_{\tau\nu}, \phi_{\tau\nu}} d \cos \theta_{\tau\nu} d\phi_{\tau\nu} \frac{d\sigma_{\nu\tau}}{dE_\tau d \cos \theta_{\tau\nu} d\phi_{\tau\nu}} \quad (4.1)
 \end{aligned}$$

where, Φ is the neutrino flux, $P_{\alpha\tau}$ is the oscillation probability from flavour $\alpha (e, \mu)$ to τ , N_T is the total number of target nuclei (50 kton iron) and T is the exposure time (5 years).

Table 2: Variation of N_τ with incident neutrino angle.

θ_ν	N_{τ^-}	N_{τ^+}	$\cos \theta_\nu$	N_{τ^-}	N_{τ^+}
$0^\circ - 90^\circ$	~ 0	~ 0	$1.0 - 0.0$	~ 0	~ 0
$90^\circ - 105^\circ$	19	8	$0.0 - -0.25$	18	8
$105^\circ - 130^\circ$	53	21	$(-0.25 - (-)0.5$	34	14
$130^\circ - 155^\circ$	34	12	$(-0.5 - (-)0.75$	34	12
$155^\circ - 180^\circ$	11	4	$(-0.75 - (-)1.0$	31	11

5. Possible experimental signatures of tau events in the ICAL detector

Direct detection of tau-leptons in the ICAL detector is not possible due to thick iron absorbers. Lifetime of tau-leptons is about 0.3 ps in its rest frame and hence, it decays very fast to other lighter leptons (e or μ) or hadrons. The hadrons produced in tau production and decay, which is expected to be identifiable over the NC hadrons background, is an indirect signature of tau events in this kind of a detector. Relevant discussion on tau decays, necessary normalisation between the present cross-sections and cross-sections from the neutrino generator, NUANCE, and final simulated results are presented in the following sections.

5.1 Tau decays

In the leptonic decay of taus the most probable energy of these leptons is peaked at the lower region of energy with respect to the input tau energy (E_τ), so these leptons can not be identified separately from direct muons coming from ν_μ CC interactions with the iron target. But their contribution as a background has to be accounted for in the oscillation analysis. This is beyond the scope of the present study. Instead, we focus on indirect tau observation through modification of the NC rate through its decay into hadrons. Now, $d\Gamma_{\tau \rightarrow \Sigma h}/dE_h$ for tau decays to hadrons are not trivial to calculate from kinematics as there are many branching modes. TAUOLA package through NUANCE interface is used to get branching ratio for tau decay to hadrons. Fixed energy ν_τ s are considered to be interacted with iron target to produce taus. Now, all type of decay modes are obtained where we choose only those decays where in the final state, no lepton (i.e., e or μ) is present. And doing so, all possible decay modes of tau to hadrons are separated. In these decays ($\tau \rightarrow \nu_\tau \Sigma h$), hadrons carry major fraction of tau energy compared to the final state ν_τ . An example plot is shown in Figure 3, where initially 16 GeV ν_τ was chosen which gives τ and then their decay to hadrons are selected to plot tau energy (E_τ), output ν_τ energy and net energy of hadrons. This figure clearly shows mean energy of hadrons is almost half of the initial decaying tau energy. As direct tau is not available to start with in TAUOLA, different set of energies for ν_τ are chosen with a large sample. Taus are selected with energies in 1 GeV bins around 4, 5, 6, 7, 8, 9 and 10 GeV. Energy of hadrons (E_h) are calculated as $E_h = E_\tau - E_{\nu_\tau}$. Scaling behaviour clearly indicates that the distribution is independent of E_τ within statistical fluctuations and only depends on the ratio E_h/E_τ (Figure 4).

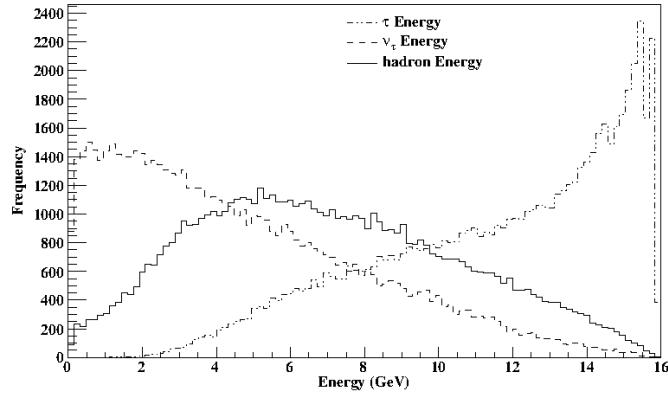


Figure 3: $\tau \rightarrow \nu_\tau h$: Energy of τ , ν_τ and net hadrons. Now, this τ is coming from ν_τ , where ν_τ energy is fixed in TAUOLA.

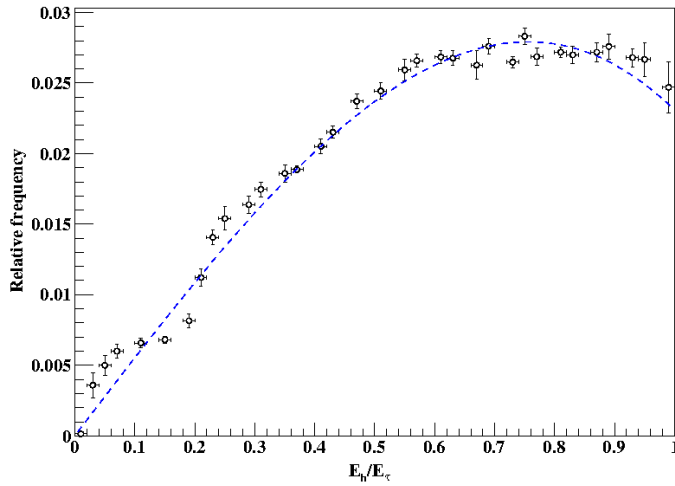


Figure 4: The profile histogram for all the energy sets with a polynomial fit of degree 3.

5.2 Normalisation due to cross-sections

Our code so far does not include the NC cross sections; hence NC events from NUANCE are considered in this study. Apart from QE and DIS, more number of processes are included in the resonance scattering inside NUANCE, whereas only the Δ resonance is considered in the present analysis. This change in the cross-sections will not make much difference as the main contribution arises from DIS events. Still, an overall normalisation is adopted to scale the total number of events. Using same cross-section code, total number of μ^\pm are estimated (as in the case for taus). Afterwards, CC events due to ν_μ (and anti-particle) interaction with the iron target which gives μ^- (and anti-particle) are looked for in NUANCE. With respect to these total number of muons, an overall normalisation is obtained as NUANCE/present code of about 1.16. So, total number of hadron events from the NC event sample from NUANCE are then scaled while comparing with the hadron events arising from tau interactions in our calculation.

5.3 Tau event generation through Monte-Carlo method

A Monte-Carlo based event generator is used to generate the kinematics of each of the tau events. This kinematics reflects the $(E_\nu, \cos\theta, \phi)$ dependence of the neutrino fluxes and the $(E_\nu, E_\tau, \cos\theta_\tau, \phi_\tau)$ dependence of the neutrino cross sections. The code is faster than the NUANCE generator since only the kinematics of the leptons is generated, not that of the hadrons.

5.4 Comparison of hadron events: tau induced hadrons and NC background

The NC process for neutrino interactions is $\nu_l + N \rightarrow \nu_l + X$, where $l : e, \mu, \tau, N$ is the nucleon and X is the hadrons in the final state. In this kind of a process, hits due to hadrons and from recoiled nucleons cannot be distinguished in the detector and together is defined as net hadrons hits. The net hadron energy is thus formally defined within the Monte Carlo code as $E_h^{NC} = E_\nu^{input} - E_\nu^{final}$. In case of tau induced hadrons, there are two sources of hadrons. One source is, $\nu_\tau + N \rightarrow \tau^- + X$, where $E_{h1} = E_\nu - E_\tau$. Another source is when tau decays to hadrons, $\tau^- \rightarrow \nu_\tau + \sum h$, where $E_{h2} = E_\tau - E_\nu$ or vector addition of all momenta of hadrons in the final state. Total of E_{h1} and E_{h2} is defined as total hadron energy (E_h) in tau events. In this study, all the particle production is strongly forward boosted. Tau leptons produced from neutrinos are very much in the forward direction (within 5° with respect to the incident neutrino) and in this process the angle between incident neutrino with the net hadron momentum vector is also peaked around 5° . The angle between tau-leptons and the net momentum vector of decayed hadrons is also peaked around 3° . So, events are very much in the forward directions with respect to the initial neutrino direction; in other words, the up-going tau neutrinos give rise to visible signals in the detector that also correspond to ‘‘up-going’’ events. In the case of NC events, the up-going and down-coming samples are separated. In each case, an angle cut near horizontal direction (5° in either direction from horizon) is applied to filter out those events which may be identified with wrong direction due to large angle scattering. Tau induced hadrons events, as obtained, are plotted with hadron events from NC event sample in the same hadron energy bin in Figure 5.

The significance of the tau contribution can be determined through a χ^2 analysis. When the ‘‘data’’ consisting of NC (up and down) and tau induced signal together are fitted to NC alone, the $\Delta\chi^2$ obtained is 59.6 so the indirect observation of tau through this channel is at more than 7σ confidence level. Hence our simulations indicate that there is an excellent possibility to detect τ events from oscillations of atmospheric neutrinos in the ICAL detector by studying the modifications of the NC signals. A more detailed analysis is required in order to obtain constraints on the neutrino oscillation parameters themselves from this channel. This is a future possible direction of study.

6. Summary

This simulation study indicates that there is a possibility to detect tau events from the oscillations of atmospheric neutrinos in the ICAL detector by studying the distortion of the NC signals due to tau production and (hadronic) decay. Developing the NC cross sections algorithm within this same framework is in progress. A more detailed analysis is required in order to obtain constraints on the neutrino oscillation parameters themselves from this channel. This is a future possible direction of study.

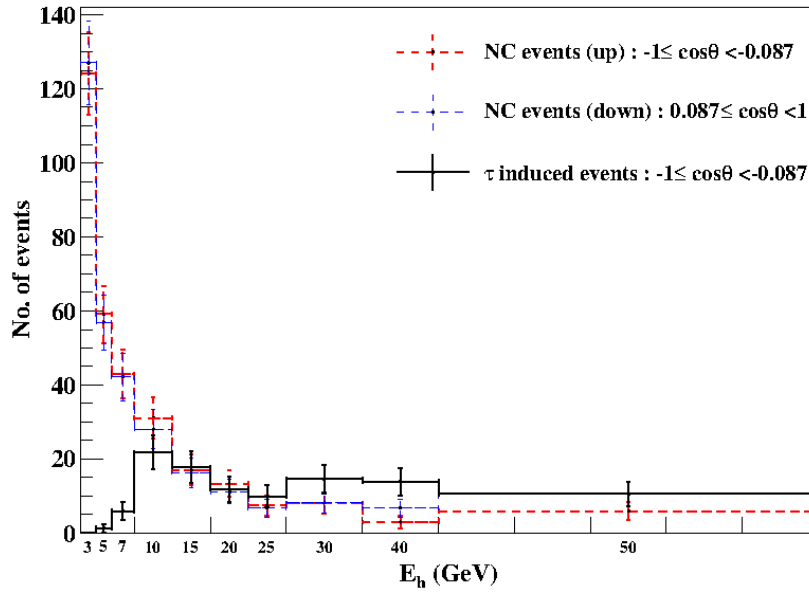


Figure 5: Number of hadron events due to NC sample and from tau induced hadrons. Here, 3 GeV bin corresponds to 3 – 5 GeV and so on, whereas the last bin corresponds to 50 – 100 GeV.

Acknowledgements

We acknowledge Prof. M.V.N Murthy and Prof. Nita Sinha for their suggestions and comments during the work. We also acknowledge the INO collaboration for various comments. Involvement of Mr. R Thiru Senthil in this work is also appreciated and acknowledged.

References

- [1] <http://www.icrr.u-tokyo.ac.jp/mhonda/>
- [2] Honda et al., *Improvement of low energy atmospheric neutrino flux calculation using the JAM nuclear interaction model*, *Phys. Rev. D* **vol 83**, **issue 12** (June, 2011).
- [3] Honda et al., *Phys. Rev. D* **75**, 043006 (2007).
- [4] Honda et al., *Phys. Rev. D* **70**, 043008 (2004).
- [5] D. Indumathi, M. V. N. Murthy, G. Rajasekaran and Nita Sinha, *Phys. Rev. D* **74**, 053004 (2006).
- [6] M. C. Gonzalez-Garcia, M. Maltoni, J. Salvado and T. Schwetz, *JHEP* **12**, (2012) 123, (arXiv:1209.3023 [hep-ph]).
- [7] A. M. Dziewonski and D. L. Anderson, *Phys. Earth Plan. Int.*, **25**, 297 (1981).
- [8] K. Hagiwara et al., *Nuclear Physics B* **668** (2003) 364-384.